ChemPubSoc Europe

DOI: 10.1002/chem.201403772

CHEMISTRY
A European Journal
Communication

Supramolecular Hydrogels

Highly Phosphorescent Supramolecular Hydrogels Based on Platinum Emitters

Naveen Kumar Allampally,[a] Michael Bredol,[b] Cristian A. Strassert,*[c] and Luisa De Cola*[d]

Abstract: We have synthesised a neutral, water-soluble, Pt^{II} complex able to aggregate more efficiently in aqueous solutions than in organic solvents. The aggregates are luminescent and are not quenched by molecular oxygen. Further, we have prepared phosphorescent hydrogels utilising host–guest interactions between cyclodextrins and the tetraethylene glycol tails of the Pt^{II} complex. The soft assemblies feature host-dependent emission properties.

Self-assembly of small molecules into new functional architectures has been object of intensive investigations in the past few years.[1] Amongst the soft assemblies, gels play an important role as materials for targeted drug delivery and tissue engineering, particularly with polymer-based gels.[2] Unfortunately, the lack of biodegradability and issues related to chemical composition come into picture as disadvantages.[3] Thus, low-molecular-weight gelators (LMWGs) have been proposed as interesting alternatives, as they can assemble forming intricate networks in different solvents and disassemble by various external stimuli.[1a,c,3,4] Amongst the different type of gelators, those able to entrap water are of particular interest, since the resulting hydrogel materials can find applications in biomedicine,[5] and they can even lead to a 3D matrix for the encapsulation of living cells.[6] The gels can also be photoactive and emissive upon either incorporation of a luminescent species, or by using emitters which act as gelators.[1c,7] Metal gelators, in particular those containing Pt^{II} chelates, are interesting due to their luminescent properties.[8] In this respect, Pt^{II} complexes and their assemblies have recently found applications in organic light emitting diodes (OLEDs),[8a,9] sensors,[10] vapochromic materials[11] and LMWGs.[8b,c,12] Indeed, organogels and hydrogels of Pt^{II} complexes have been reported in which electrostatic and/or π–π interactions played a fundamental role.[8f,13] However, most of the hydrogels turned out to be non-luminescent, most probably due to quenching of the long-lived phosphorescence by molecular dioxygen. Furthermore, luminescent hydrogel matrices have been prepared by employing f-block metal cations (3+) and sodium cholate, but without displaying reversibility to sols.[14]

In many cases, the stability of the hydrogel is a problem and a way to induce the formation of a strong gelating network is to take advantage of host–guest interactions. Cyclodextrin (CD) constitutes a water-soluble building block able to act as a host. Indeed, the self-assembly of polyethylene glycol (PEG) and α-CD was firstly reported by Harada et al.[15] They showed that α-CD can assist the organisation by hosting PEG chains. Following this approach, other hydrogels and self-assembled structures that display reversible assembly and disassembly upon external inputs have been described.[16] Therefore, an interesting combination of luminescent and stable gels can be obtained with phosphorescent Pt^{II} complexes possessing one of these two components (PEG or CD) and adding the complementary guest or host in order to create phosphorescent hydrogels. However, Pt^{II} complexes can be quenched by the dioxygen present in the solvent, and therefore must be protected to avoid bimolecular interactions. In this respect, we have recently reported the aggregation-induced emission (AIE) of a Pt^{II} compound bearing a dianionic tridentate ligand[8a] and, also shown that appropriate ancillary ligands facilitate the gelation of solvents of different polarity, such as dichloromethane (DCM) and dimethylformamide (DMF).[8i]

In the present work, we have tuned the structure in order to make it water soluble by attaching two tetraethylene glycol (TEG) chains on the ancillary ligand (Scheme 1, **1**–**4**), while keeping the chromophoric tridentate chelate unaffected. The

---

[a] Dr. N. K. Allampally
NRW Graduate School of Chemistry
Westfälische Wilhelms-Universität Münster
Wilhelm-Klemm-Str.10, 48149 Münster (Germany)
and
Center for Nanotechnology (CeNTech) and Physikalisches Institut
Westfälische Wilhelms-Universität Münster.
Heisenbergstr. 11, 48149 Münster (Germany)
Current address:
Institut für Organische Chemie, Universität Würzburg
Am Hubland, 97074 Würzburg (Germany)

[b] Prof. Dr. M. Bredol
Department of Chemical Engineering
Münster University of Applied Sciences
Stegerwaldstr. 39, 48565 Steinfurt (Germany)

[c] Dr. C. A. Strassert
Center for Nanotechnology (CeNTech) and Physikalisches Institut
Westfälische Wilhelms-Universität Münster
Heisenbergstr. 11, 48149 Münster (Germany)
E-mail: ca.s@wwu.de

[d] Prof. L. De Cola
Center for Nanotechnology (CeNTech) and Physikalisches Institut
Westfälische Wilhelms-Universität Münster
Heisenbergstr. 11, 48149 Münster (Germany)
Current address:
Institut de Science et d'Ingénierie Supramoléculaires
Université de Strasbourg, 8 Allée Gaspard Monge
67000 Strasbourg (France)
E-mail: decola@unistra.fr

Supporting information for this article is available on the WWW under http://dx.doi.org/10.1002/chem.201403772.

© 2014 Wiley-VCH Verlag GmbH & Co. KGaA, Weinheim

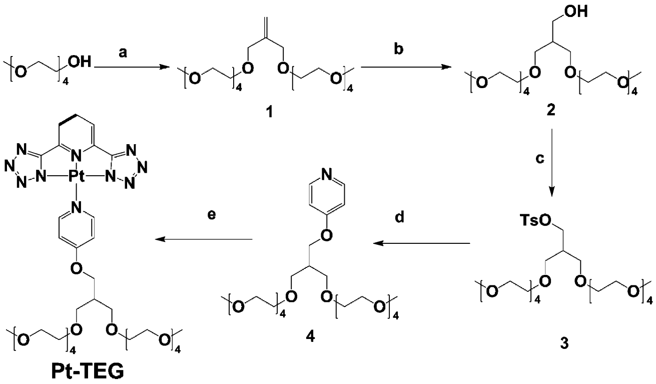

Scheme 1. Synthesis of complex **Pt-TEG**, a) NaH, dry THF, 3-chloro-2-(chloromethyl)prop-1-ene, from room temperature (RT) to 65 °C, overnight (90% yield); b) BH_3·THF stir at 0 °C for 3 h, NaOH-H_2O_2, stir at RT for 1.5 h (85% yield); c) Ag_2O, tosyl chloride, KI, DCM, RT, 2 h (75% yield), d) 4-hydroxypyridine, K_2CO_3, CH_3CN, reflux, 48 h (75% yield) and e) $[Pt(dmso)_2Cl_2]$, 2,6-bis-(tetrazole-5-yl)pyridine, DIPEA, CH_3CN, reflux under N_2 overnight (yield 60%).

resulting complex, **Pt-TEG** (Scheme 1), can form hydrogels upon interaction of the TEG chains with CDs. Interestingly, due to the self-assembly of the complex, phosphorescence is observed in water. Furthermore, we demonstrate that the luminescence of the resulting hydrogels can be tuned by changing the size of the CD host (α- or β-CD). The synthesis, characterisation, photophysical, rheological and morphological properties are described herein.

The complex **Pt-TEG** was prepared by reacting the ancillary ligand **4** and 2,6-bis(tetrazole-5-yl)pyridine with $[Pt(dmso)_2Cl_2]$ (Scheme 1). The compound was purified by column chromatography and characterised by ^1H and ^{13}C NMR spectroscopy, HR-MS and elemental analysis. Solvent-dependent ^1H NMR studies confirmed the aggregation phenomena evidenced by the photophysical properties (vide infra). Indeed, the aromatic signals (doublets in CD_2Cl_2) collapse into broad bands in D_2O (Figure S1 in the Supporting Information). Furthermore, the aromatic signals are broadened and shifted to higher fields when compared to CD_2Cl_2, which indicates that the aromatic (hydrophobic) part is mainly responsible for the aggregation process induced by π–π interactions. Thus, the aromatic protons are shifted up-field upon aggregation, whereas the signals of the TEG chains are barely displaced and remain essentially unaffected in terms of multiplicity (Figure S1 in the Supporting Information).

The room-temperature absorption spectra of **Pt-TEG** in DCM (Figure S2 in the Supporting Information) and in water (Figure 1) display an ancillary pyridine- and a tridentate-ligand-centred (^{1}LC) π–π* transition (310 and 340 nm, respectively), as well as the characteristic, lower energy, metal-to-ligand charge-transfer (^{1}MLCT) bands (360–400 nm).[8a,i] Comparing solutions of increasing concentration (between 10^{-5} and 10^{-3} м), the rise of a new absorption band at 430 nm can be observed above 10^{-4} м, and can be assigned to a metal-to-metal-to-ligand charge-transfer (^{1}MMLCT) absorption band, which clearly points towards ground state aggregation equilibria. This is supported by the clear deviations from linearity when the absorbance is plotted against the concentration (Figure 1 in water and Figure S3 in DCM in the Supporting Information). Consistently, only above 10^{-4} м, the emission of these aggregates was observed at 590 nm in DCM and at 580 nm in water, and can be assigned to a radiative transition from a ^{3}MMLCT state. The emission of the monomeric form was not observed at room temperature. The excitation spectra obtained by monitoring the emission of the aggregates reproduce the band at 430 nm (Figure 2).

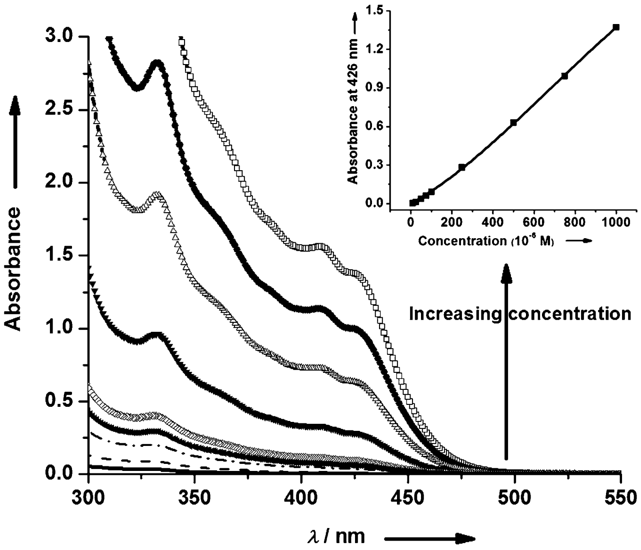

Figure 1. Concentration-dependent absorption spectra of **Pt-TEG** in water at RT (0.01, 0.025, 0.05, 0.075, 0.1, 0.25, 05, 0.75 and 1 mм). Inset: Lambert–Beer plot with nonlinear fit.

The emission of **Pt-TEG** is red-shifted from 550 nm in neat films to 590 nm in fluid DCM (Figure 2 and Figure S4 in the Supporting Information), due to the stabilisation of the emissive CT state by the solvent. However, we observe a subtle yet clear blue-shift of the luminescence when going from DCM to

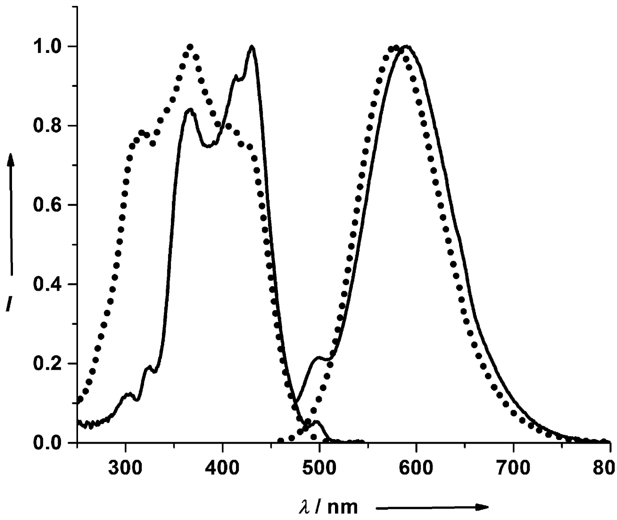

Figure 2. Excitation (left, $\lambda_{em} = 580$ or 590 nm) and emission (right, $\lambda_{ex} = 430$ nm) of 10^{-4} м **Pt-TEG** at RT in aerated DCM (—) and water (···).

water. A slightly increased Pt–Pt distance due to an enhanced solvation of the hydrophilic TEG tails in the periphery of the aggregates accounts for this observation. As water solvates the hydrophilic TEG tails more efficiently than DCM, it increases the separation between the Pt^{II} centres, causing a concomitant blue-shift. Bredas et al.[17] have recently shown that the properties of triplet excimers of Pt^{II} complexes strongly depend on their relative orientation, and the resulting Pt–Pt distances and π–π stacking. Thus, we cannot exclude a different packing in the two solvents, leading in DCM to a *syn*-orientation between two adjacent complexes (both tridentate ligands on top of each other), and an *anti*-configuration in water (with the tridentate ligand on top of the pyridine). Indeed, the observed augmentation of the radiative rate constant (Table 1) also points towards a higher transition dipole moment. Thus, a fourfold enhancement of the luminescence quantum yield is obtained in water, as compared to DCM. Such enhancement of the radiative process indicates that the above-mentioned different relative orientations and their effect on the excited state are mostly responsible for the variation of the transition dipole moments.

The emission and excitation spectra of **Pt-TEG** at 77 K were measured in 2-methyltetrahydrofuran (2-MeTHF) (Figure S4 in the Supporting Information). The emission of the monomer and the aggregates were both observed, depending on the excitation wavelength. Upon excitation in the UV ($\lambda_{ex}=330$ nm), we observed predominant deep-blue emission ($\lambda_{em}=420$ nm) with a clear vibrational progression that can be assigned to the phosphorescence from the metal-perturbed ligand-centred excited triplet state (^{3}LC) of the monomeric species, and a weaker unstructured luminescence ($\lambda_{em}=570$ nm) similar to the room-temperature emission of the aggregated species, which is attributed to a ^{3}MMLCT state. As expected, due to the CT character, the emission of the aggregates in a rigid matrix at 77 K is blue-shifted as compared to fluid solution. Excited state lifetimes confirm these assignments.[8i] Monitoring the emission at 420 or 450 nm, the long ^{3}LC decay (ca. 13 μs) is observed. At 570 nm, the emission decay shows a shorter-lived ^{3}MMLCT component (ca. 4 μs) (Table 1).

The **Pt-TEG** complex self-assembles into discrete aggregates at higher concentrations in water, rather than forming a gelating network. Indeed, dynamic light scattering (DLS) measurements (Figure S5 a in the Supporting Information) and transmission electron microscopy (TEM) (Figure S5 b–d in the Supporting Information) revealed that above 1 mᴍ, **Pt-TEG** assembles into amorphous structures of variable size. The DLS measurements showed two distributions, one below 6 nm that can be assigned to the smaller aggregates observed in the TEM (Figure S5 b–d), and one between 30 and 300 nm related to the larger assemblies.

To favour the gelation process in water, CDs were added to induce host–guest interactions between the TEG chains of the complex and the hydrophobic cavity of the CDs. In order to obtain stable gels, the minimum molar concentration ratio between **Pt-TEG** and CDs is 1:7 (Table 2). Interestingly, α- and β-CDs gave stable gels (Figure 3 a, b, e and f), whereas no gelation was observed with γ-CD (Figure S7 in the Supporting Information), most likely due to the size mismatch between the TEG tails and the cavity.[15b] In the case of α- or β-CD, one CD unit forms a host–guest complex with one ethylene oxide segment.[15] As the **Pt-TEG** complex bears two tetraethylene glycol moieties, up to four CD molecules can be bound to one molecule of **Pt-TEG**. The excess of three CD molecules is probably required for hydrogen bonding between the host–guest com-

Table 2. Composition of hydrogels.

Hydrogel	Guest (**Pt-TEG**) [mg]	Host (CD) [mg]	Volume of water [μL]
α-hydrogel	16.5	117	250
β-hydrogel	16.6	120	250

Table 1. Photophysical data of Pt-TEG.

	τ [μs][c]	λ_{em} [nm]	Φ (×100)	k_r [10^6 s^{-1}]	k_{nr} [10^{-6} s^{-1}]
DCM[a]	0.040 (74 %), 0.154 (26 %)	590	0.07[d]	0.01	14.48
DCM[b]	0.038 (74 %), 0.145 (26 %)	590	0.07[d]	0.01	15.4
water	0.017 (81 %), 0.058 (19 %)	580	0.26[d]	0.105	40.25
neat film	0.513	550	19.73[f]	0.385	1.56
α-hydrogel	0.219 (62 %), 0.382 (38 %)	558	6.65[e]	0.237	3.32
β-hydrogel	0.126 (67 %), 0.384 (33 %)	580	4.60[e]	0.22	4.53
α-xerogel	0.285 (39 %), 0.567 (61 %)	555	18.05[e]	0.39	1.8
β-xerogel	0.511	555	26.85[e]	0.525	1.43
2-MeTHF, 77 K ($\lambda_{ex}=435$ nm, $\lambda_{em}=570$ nm)	3.89 (90 %), 11.58 (10 %)	570	–	–	–
2-MeTHF, 77 K ($\lambda_{ex}=365$ nm, $\lambda_{em}=570$ nm)	3.99 (91 %), 12.90(9 %)	570	–	–	–
2-MeTHF, 77 K ($\lambda_{ex}=330$ nm, $\lambda_{em}=570$ nm)	4.07(87 %), 12.85(13 %)	570	–	–	–
2-MeTHF, 77 K ($\lambda_{ex}=365$ nm, $\lambda_{em}=450$ nm)	12.96	570, 420, 450	–	–	–
2-MeTHF, 77 K ($\lambda_{ex}=365$ nm, $\lambda_{em}=420$ nm)	13.05	570, 420, 450	–	–	–
2-MeTHF, 77 K ($\lambda_{ex}=330$ nm, $\lambda_{em}=450$ nm)	12.65	570, 420, 450	–	–	–
2-MeTHF, 77 K ($\lambda_{ex}=330$ nm, $\lambda_{em}=420$ nm)	12.88	570, 420, 450	–	–	–

[a] Deaerated. [b] Aerated. [c] Relative amplitudes are given in brackets. [d] Quantum yields determined using $[Ru(bpy)_3Cl_2]\cdot xH_2O$ as a reference ($\lambda_{ex}=390$ nm).[18] [e] Quantum yields measured using an integrating sphere ($\lambda_{ex}=445$ nm). [f] Quantum yields measured using an integrating sphere, averaging between $\lambda_{ex}=330$ nm and $\lambda_{ex}=430$ nm.

© 2014 Wiley-VCH Verlag GmbH & Co. KGaA, Weinheim

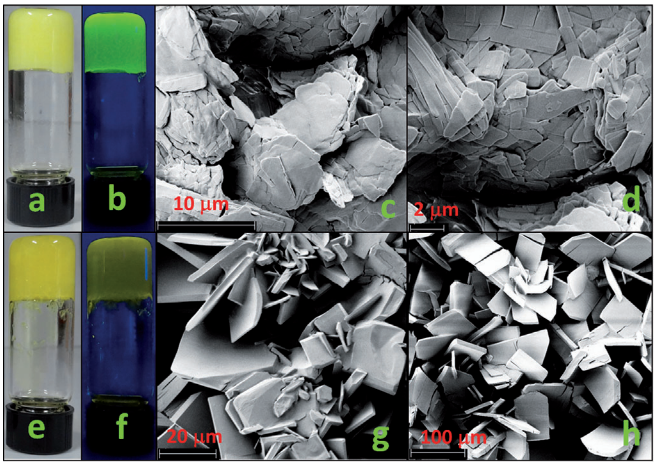

Figure 3. α-hydrogel a) under day light and b) UV-light; c) and d) are SEM images of the α-xerogel. β-hydrogel under e) day light and f) UV-light; g) and h) are SEM images of the β-xerogel.

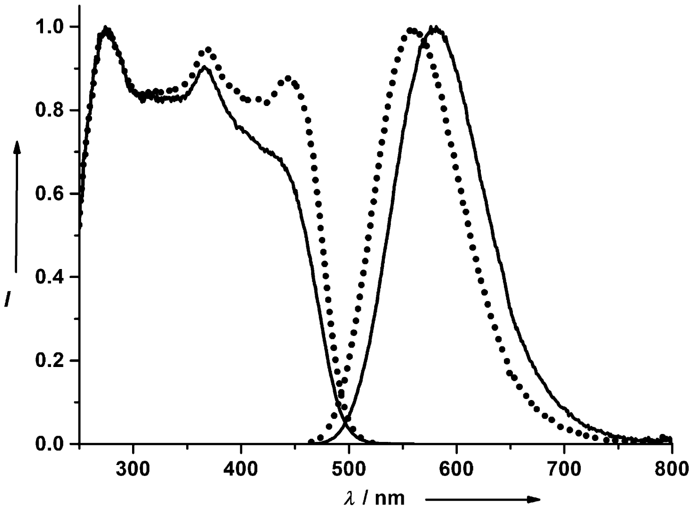

Figure 4. Left: Excitation spectra ($\lambda_{em} = 555$ nm or $\lambda_{em} = 580$ nm for α- and β-hydrogels, respectively); right: emission spectra ($\lambda_{ex} = 445$ nm) of α-hydrogel (···) and β-hydrogel (—).

plexes and with water, which ultimately stabilises the hydrogels (Figure S8 in the Supporting Information). The hydrogels showed emissions in the visible part of the electromagnetic spectrum (Figure 4) that depend on the CD employed for the gelation. The α-hydrogel emission ($\lambda_{max} = 558$ nm) is strongly blue-shifted as compared to the β-hydrogel ($\lambda_{max} = 580$ nm), whereas the radiative rate constant remains essentially unaffected (Table 1). The fact that the radiative process is not influenced indicates that the nature of the emissive state is essentially the same in both cases. Thus, a comparable relative orientation of the aggregated complexes is expected. Indeed, in the absence of water, the radiative rate constants of the xerogels are comparable with the ones of the hydrogels, whereas the non-radiative deactivation is significantly prevented due to the higher rigidity of the environment in the absence of solvent. Thus, it is clear that the accessibility to water and the resulting solvation of the emissive aggregates is less efficient in the α-hydrogel than in the β-hydrogel, thus shifting the luminescence to higher energies at which the xerogels also emit ($\lambda_{max} = 550$ nm). Indeed, the emission wavelengths of both xerogels (Figure 3 c, d, g and h) are similar to the neat films of pure **Pt-TEG**, due to the complete lack of solvent stabilisation of the emissive excited state (Table 1 and Figure S6 in the Supporting Information). The excited state lifetime of the β-xerogel and the neat film are the same, whereas those of the α-xerogel are of the same order of magnitude, but bi-exponential in nature (Table 1). The β-xerogel reaches the highest photoluminescence quantum yield (PLQY), namely 27 %, whereas the α-xerogel is somewhat less luminescent (PLQY = 18 %).

Both hydrogels are stable at room temperature for several days, and display reversible sol–gel transitions for several times upon heating to 70–80 °C and leaving at room temperature for 10–15 min. A rheological characterisation was carried out for the α-hydrogel, whereas the β-hydrogel appears too grainy for reliable measurements. A stress amplitude sweep at 25 °C under oscillating deformation at 1 Hz showed that the elastic part of the shear modulus (G') remains dominant by about two orders of magnitude over the viscous part (G''), up to very high stress amplitudes (ca. 200 Pa), thus pointing to a quite rigid underlying three-dimensional structure (Figure 5 a). In measurements in which the gap between cone and plate of the rheometer was filled only in the region around the cone tip (in order to avoid problems with sample slip at high stress amplitudes), G' and G'' are demonstrated to be clearly correlated with each other (as expected by the Kramers–Kronig relations), showing the consistency of the rheological data (Figure S9 in the Supporting Information).

For stationary flow, conditions for mechanical breakdown of the gel can be interpreted as yield stress. In systems with strong interaction, flow beyond yield stress often follows a power law (Ostwald–de Waele equation). In Figure S10 in the Supporting Information, the absolute value of the complex viscosity of the α-hydrogel (as measured in Figure S9 in the Supporting Information) is plotted over the stress amplitude in that region only, that is, the part dominated by the viscous part of the modulus, G''. The data can be fitted to a power law with an exponent typical for shear-thinning behaviour. This demonstrates again that the structure of the α-hydrogel is dominated by strong local interactions. However, once the α-hydrogel is destroyed by mechanical stress, it recovers from its fluid state only slowly, but not to the previous strength; this can be restored only through thermal cycling via the sol state. Amplitude sweeps after mechanical breakdown showed gel-like elastic behaviour (G' is much larger then G''), but not with the same high values of G' as previously observed, and without being resistant against high stress levels as before (Figure 5 b). The gels obtained by recovery after breakdown at room temperature are evidently weaker than the freshly prepared ones by cooling from the sol state. It thus appears that the mobility of the constituents at room

© 2014 Wiley-VCH Verlag GmbH & Co. KGaA, Weinheim

⇖⇖ These are not the final page numbers!

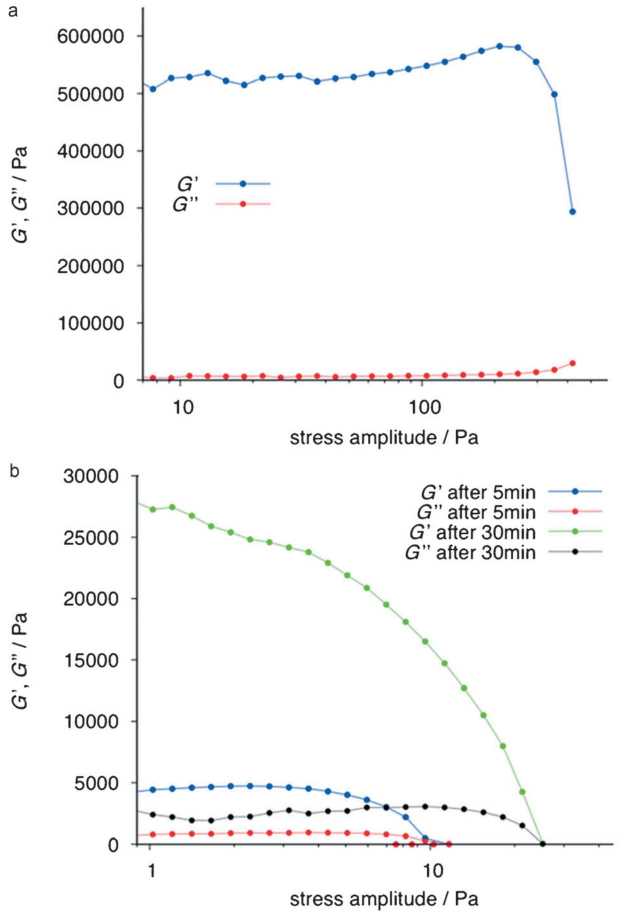

Figure 5. a) Amplitude sweep of the α-hydrogel, and b) amplitude sweeps of the α-hydrogel after mechanical breakdown (loss of elastic nature by mechanical stress); time elapsed after breakdown according to the legend.

temperature is too small to enable the complete self-reassembly of the α-hydrogel.

In summary, our strategy combines the versatility of supramolecular self-assemblies with the tuneable multi-centred phosphorescence of Pt^{II} complexes within a soft architecture. The sensitivity of the luminescence towards structural variations paves a new way for the design of water-processable functional materials with optical and sensing properties for technological and biomedical applications.

Acknowledgements

N. K. Allampally acknowledges the NRW Graduate School of Chemistry (NRW GSC-MS) for doctoral fellowship. We acknowledge Dr. Henning Lülf for the SEM images.

Keywords: aggregation · host–guest systems · hydrogels · phosphorescence · platinum

[1] a) L. A. Estroff, A. D. Hamilton, *Chem. Rev.* **2004**, *104*, 1201 – 1218; b) S. S. Babu, S. Prasanthkumar, A. Ajayaghosh, *Angew. Chem. Int. Ed.* **2012**, *51*, 1766 – 1776; *Angew. Chem.* **2012**, *124*, 1800 – 1810; c) M. O. Piepenbrock, G. O. Lloyd, N. Clarke, J. W. Steed, *Chem. Rev.* **2010**, *110*, 1960 – 2004; d) C. A. Palma, M. Cecchini, P. Samori, *Chem. Soc. Rev.* **2012**, *41*, 3713 – 3730; e) G. M. Whitesides, B. Grzybowski, *Science* **2002**, *295*, 2418 – 2421; f) J. M. Lehn, *Proc. Natl. Acad. Sci. USA* **2002**, *99*, 4763 – 4768; g) D. Philp, J. F. Stoddart, *Angew. Chem. Int. Ed. Engl.* **1996**, *35*, 1154 – 1196; *Angew. Chem.* **1996**, *108*, 1242 – 1286; h) G. V. Oshovsky, D. N. Reinhoudt, W. Verboom, *Angew. Chem. Int. Ed.* **2007**, *46*, 2366 – 2393; *Angew. Chem.* **2007**, *119*, 2418 – 2445; i) W. Li, Y. Kim, M. Lee, *Nanoscale* **2013**, *5*, 7711 – 7723; j) E. Busseron, Y. Ruff, E. Moulin, N. Giuseppone, *Nanoscale* **2013**, *5*, 7098 – 7140; k) A. R. Hirst, B. Escuder, J. F. Miravet, D. K. Smith, *Angew. Chem. Int. Ed.* **2008**, *47*, 8002 – 8018; *Angew. Chem.* **2008**, *120*, 8122 – 8139.

[2] a) Y. Q. Liang, Y. Qiao, S. T. Guo, L. Wang, C. P. Xie, Y. L. Zhai, L. D. Deng, A. J. E. Dong, *Soft Matter* **2010**, *6*, 1915 – 1922; b) J. K. Oh, *Soft Matter* **2011**, *7*, 5096 – 5108; c) M. H. Park, M. K. Joo, B. G. Choi, B. Jeong, *Acc. Chem. Res.* **2012**, *45*, 424 – 433; d) I. Tomatsu, K. Peng, A. Kros, *Adv. Drug Delivery Rev.* **2011**, *63*, 1257 – 1266.

[3] W. T. Truong, Y. Su, J. T. Meijer, P. Thordarson, F. Braet, *Chem. Asian J.* **2011**, *6*, 30 – 42.

[4] a) X. Y. Yang, G. X. Zhang, D. Q. Zhang, *J. Mater. Chem.* **2012**, *22*, 38 – 50; b) H. Maeda, *Chem. Eur. J.* **2008**, *14*, 11274 – 11282; c) J. H. van Esch, *Langmuir* **2009**, *25*, 8392 – 8394; d) S. S. Babu, V. K. Praveen, A. Ajayaghosh, *Chem. Rev.* **2014**, *114*, 1973 – 2129; e) G. Yu, X. Yan, C. Han, F. Huang, *Chem. Soc. Rev.* **2013**, *42*, 6697 – 6722; f) N. M. Sangeetha, U. Maitra, *Chem. Soc. Rev.* **2005**, *34*, 821 – 836.

[5] Z. Yang, G. Liang, B. Xu, *Acc. Chem. Res.* **2008**, *41*, 315 – 326.

[6] a) Z. Huang, H. Lee, E. Lee, S. K. Kang, J. M. Nam, M. Lee, *Nat. Commun.* **2011**, *2*, 459; b) C. Yang, D. Li, Z. Liu, G. Hong, J. Zhang, D. Kong, Z. Yang, *J. Phys. Chem. B* **2012**, *116*, 633 – 638; c) S. Zhang, M. A. Greenfield, A. Mata, L. C. Palmer, R. Bitton, J. R. Mantei, C. Aparicio, M. O. de La Cruz, S. I. Stupp, *Nat. Mater.* **2010**, *9*, 594 – 601; d) E. C. Wu, S. Zhang, C. A. E. Hauser, *Adv. Funct. Mater.* **2012**, *22*, 456 – 468.

[7] a) J. W. Steed, *Chem. Commun.* **2011**, *47*, 1379 – 1383; b) G. De Paoli, Z. Džolic, F. Rizzo, L. De Cola, F. Vögtle, W. M. Müller, G. Richardt, M. Žinic, *Adv. Funct. Mater.* **2007**, *17*, 821 – 828; c) Y. Qiao, Y. Lin, S. Zhang, J. Huang, *Chem. Eur. J.* **2011**, *17*, 5180 – 5187; d) P. K. Sukul, D. Asthana, P. Mukhopadhyay, D. Summa, L. Muccioli, C. Zannoni, D. Beljonne, A. E. Rowan, S. Malik, *Chem. Commun.* **2011**, *47*, 11858 – 11860; e) A. Kishimura, T. Yamashita, T. Aida, *J. Am. Chem. Soc.* **2005**, *127*, 179 – 183.

[8] a) C. A. Strassert, C. H. Chien, M. D. Galvez Lopez, D. Kourkoulos, D. Hertel, K. Meerholz, L. De Cola, *Angew. Chem. Int. Ed.* **2011**, *50*, 946 – 950; *Angew. Chem.* **2011**, *123*, 976 – 980; b) A. Y. Tam, K. M. Wong, V. W. Yam, *J. Am. Chem. Soc.* **2009**, *131*, 6253 – 6260; c) K. C. Chang, J. L. Lin, Y. T. Shen, C. Y. Hung, C. Y. Che, S. S. Sun, *Chem. Eur. J.* **2012**, *18*, 1312 – 1321; d) W. Lu, Y. C. Law, J. Han, S. S. Chui, D. L. Ma, N. Zhu, C. M. Che, *Chem. Asian J.* **2008**, *3*, 59 – 69; e) J. Zhang, X.-D. Xu, L.-J. Chen, Q. Luo, N.-W. Wu, D.-X. Wang, X.-L. Zhao, H.-B. Yang, *Organometallics* **2011**, *30*, 4032 – 4038; f) J. Wang, Y. Chen, Y. C. Law, M. Li, M. X. Zhu, W. Lu, S. S. Chui, N. Zhu, C. M. Che, *Chem. Asian J.* **2011**, *6*, 3011 – 3019; g) M. Mydlak, M. Mauro, F. Polo, M. Felicetti, J. Leonhardt, G. Diener, L. De Cola, C. A. Strassert, *Chem. Mater.* **2011**, *23*, 3659 – 3667; h) C. Cebrián, M. Mauro, D. Kourkoulos, P. Mercandelli, D. Hertel, K. Meerholz, C. A. Strassert, L. De Cola, *Adv. Mater.* **2013**, *25*, 437 – 442; i) N. K. Allampally, C. A. Strassert, L. De Cola, *Dalton Trans.* **2012**, *41*, 13132 – 13137.

[9] A. Y. Tam, D. P. Tsang, M. Y. Chan, N. Zhu, V. W. Yam, *Chem. Commun.* **2011**, *47*, 3383 – 3385.

[10] a) V. W. Yam, K. H. Chan, K. M. Wong, N. Zhu, *Chem. Eur. J.* **2005**, *11*, 4535 – 4543; b) K. M. Wong, V. W. Yam, *Acc. Chem. Res.* **2011**, *44*, 424 – 434.

[11] J. R. Kumpfer, S. D. Taylor, W. B. Connick, S. J. Rowan, *J. Mater. Chem.* **2012**, *22*, 14196.

[12] a) N. Komiya, T. Muraoka, M. Iida, M. Miyanaga, K. Takahashi, T. Naota, *J. Am. Chem. Soc.* **2011**, *133*, 16054 – 16061; b) A. Y. Tam, K. M. Wong, N. Zhu, G. Wang, V. W. Yam, *Langmuir* **2009**, *25*, 8685 – 8695; c) Y. Li, A. Y. Tam, K. M. Wong, W. Li, L. Wu, V. W. Yam, *Chem. Eur. J.* **2011**, *17*, 8048 – 8059; d) T. Cardolaccia, Y. Li, K. S. Schanze, *J. Am. Chem. Soc.* **2008**, *130*, 2535 – 2545; e) C. A. Strassert, M. Mauro, L. De Cola in *Photophysics of soft and hard molecular assemblies based on luminescent complexes, Vol. 63* Academic Press, **2011**, pp. 47 – 103.

[13] a) W. Lu, Y. Chen, V. A. Roy, S. S. Chui, C. M. Che, *Angew. Chem. Int. Ed.* **2009**, *48*, 7621 – 7625; *Angew. Chem.* **2009**, *121*, 7757 – 7761; b) X.-S. Xiao, W. Lu, C.-M. Che, *Chem. Sci.* **2014**, *5*, 2482 – 2488; c) C. Rest, M. J.

Mayoral, K. Fucke, J. Schellheimer, V. Stepanenko, G. Fernandez, *Angew. Chem. Int. Ed.* **2014**, *53*, 700–705; *Angew. Chem.* **2014**, *126*, 716–722.

[14] S. Banerjee, R. Kandanelli, S. Bhowmik, U. Maitra, *Soft Matter* **2011**, *7*, 8207–8215.

[15] a) A. Harada, J. Li, M. Kamachi, *Nature* **1992**, *356*, 325–327; b) A. Harada, J. Li, M. Kamachi, *Nature* **1994**, *370*, 126–128; c) A. Harada, M. Okada, J. Li, M. Kamachi, *Macromolecules* **1995**, *28*, 8406–8411; d) A. Harada, M. Kamachi, *Macromolecules* **1990**, *23*, 2821–2823.

[16] a) S. Tamesue, Y. Takashima, H. Yamaguchi, S. Shinkai, A. Harada, *Angew. Chem. Int. Ed.* **2010**, *49*, 7461–7464; *Angew. Chem.* **2010**, *122*, 7623–7626; b) Y. Yan, H. Wang, B. Li, G. Hou, Z. Yin, L. Wu, V. W. Yam, *Angew. Chem. Int. Ed.* **2010**, *49*, 9233–9236; *Angew. Chem.* **2010**, *122*, 9419–9422; c) T. Ogoshi, Y. Takashima, H. Yamaguchi, A. Harada, *J. Am. Chem. Soc.* **2007**, *129*, 4878–4879; d) Y. Takashima, T. Nakayama, M. Miyauchi, Y. Kawaguchi, H. Yamaguchi, A. Harada, *Chem. Lett.* **2004**, *33*, 890–891; e) W. Deng, H. Yamaguchi, Y. Takashima, A. Harada, *Angew. Chem. Int. Ed.* **2007**, *46*, 5144–5147; *Angew. Chem.* **2007**, *119*, 5236–5239; f) Y. Wang, N. Ma, Z. Wang, X. Zhang, *Angew. Chem. Int. Ed.* **2007**, *46*, 2823–2826; *Angew. Chem.* **2007**, *119*, 2881–2884; g) Y. Wang, H. Xu, X. Zhang, *Adv. Mater.* **2009**, *21*, 2849–2864.

[17] D. Kim, J. L. Bredas, *J. Am. Chem. Soc.* **2009**, *131*, 11371–11380.

[18] H. Ishida, S. Tobita, Y. Hasegawa, R. Katoh, K. Nozaki, *Coord. Chem. Rev.* **2010**, *254*, 2449–2458.

Received: June 1, 2014

Published online on ■■ ■■, 0000

COMMUNICATION

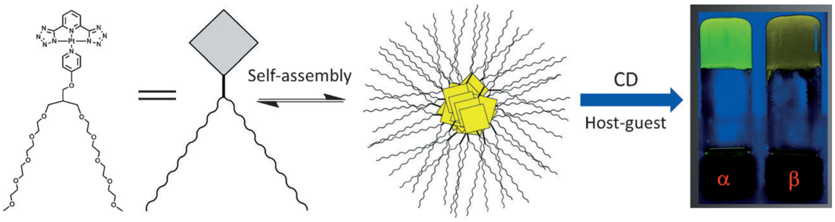

Light and sweet! Phosphorescent hydrogels based on a Pt^{II} emitter (guest) and cyclodextrins (α- and β-CD; host) are presented. The resulting soft assemblies feature host-dependent emission properties.

Supramolecular Hydrogels

N. K. Allampally, M. Bredol, C. A. Strassert, L. De Cola**

■■ – ■■

Highly Phosphorescent Supramolecular Hydrogels Based on Platinum Emitters

© 2014 Wiley-VCH Verlag GmbH & Co. KGaA, Weinheim

These are not the final page numbers! ↗↗